

1 Verification of Malkin's theorem and report of
2 problem in Figure 10-26, panel $I_{Nap} + I_K$ -model
3 (Class 2), and in Figure 10-30a, of Izhikevich
4 (2007)

5 Joaquín Rapela*

6 August 5, 2018

7 Contents

| | | |
|----|--|----------|
| 8 | 1 Introduction | 1 |
| 9 | 2 Malkin's Theorem | 1 |
| 10 | 3 Two successive simplifications and one example of Malkin's the- | |
| 11 | orem | 2 |
| 12 | 4 Problem in Figure 10-26, Panel $I_{Nap} + I_K$-model (Class 2), and in | |
| 13 | Figure 10-30a, of Izhikevich (2007), and Verification of Malkin's | |
| 14 | Theorem | 7 |

15 1 Introduction

16 Below I state Malkin's theorem, following Theorem 9.2 in Hoppensteadt & Izhikevich
17 (1997) (Section 2), present two successive simplification and one example of this
18 theorem (Section 3), report a problem in Figure 10-26, panel $I_{Nap} + I_K$ -model
19 (Class 2), and in Figure 10-30a, of Izhikevich (2007), and verify the validity of
20 Malkin's theorem (Section 4)

21 2 Malkin's Theorem

22 The following statement of Malkin's theorem is a modification of that given in
23 Theorem 9.2 of Hoppensteadt & Izhikevich (1997).

*rapela@ucsd.edu

²⁴ **Theorem 1.** Let $\mathbf{X}_i(t) \in \mathfrak{R}^m, i = 1, \dots, n$, be weakly-connected m -dimensional
²⁵ dynamical systems

$$\dot{\mathbf{X}}_i = F_i(\mathbf{X}_i) + \epsilon G_i(\mathbf{X}) \quad (1)$$

²⁶ where $\mathbf{X}(t_1, \dots, t_n) = (\mathbf{X}_1(t_1), \dots, \mathbf{X}_n(t_n)) \in \mathfrak{R}^{m \times n}$. Assume that each uncou-
²⁷ pled system

$$\dot{\mathbf{X}}_i = F_i(\mathbf{X}_i)$$

²⁸ is on a limit cycle of length T parametrized by $\gamma_i : S^1 \rightarrow \mathfrak{R}^m, \gamma_i(\theta_i) = \mathbf{X}_i(\theta_i)$.
²⁹ Define $\gamma(\theta_1, \dots, \theta_n) = (\gamma_1(\theta_1), \dots, \gamma_n(\theta_n))$, and let φ_i be the phase deviation of
³⁰ \mathbf{X}_i (i.e., $\theta_i = (t + \varphi_i) \bmod T$). Then

$$\dot{\varphi}_i = H_i(\boldsymbol{\varphi} - \varphi_i, \epsilon) \quad (2)$$

³¹ with $\boldsymbol{\varphi} - \varphi_i = (\varphi_1 - \varphi_i, \dots, \varphi_n - \varphi_i)$, and

$$H_i(\boldsymbol{\varphi} - \varphi_i, 0) = \frac{1}{T} \int_0^T Q_i(\theta)^T G_i(\gamma(\theta + \boldsymbol{\varphi} - \varphi_i)) d\theta \quad (3)$$

³² where $Q_i(\theta)$ is the solution of

$$\dot{Q}_i(\theta) = (DF_i(\gamma_i(\theta)))^T Q_i(\theta)$$

³³ satisfying the normalization condition

$$Q_i(0)^T DF_i(\gamma_i(0)) = 1$$

³⁴ with DF_i being the differential of F_i .

³⁵ **Note 1** It is remarkable that it is possible to build an n -dimensional dynamical
³⁶ model of the phase of a system (Eq. 2) from an $n \times m$ -dimensional dynamical
³⁷ model of the original system (Eq. 1).

³⁸ **3 Two successive simplifications and one exam-** ³⁹ **ple of Malkin's theorem**

⁴⁰ **Simplification 1**

⁴¹ **Lemma 1.** If in Eq. 1 the coupling term of oscillator i (G_i) is the sum of
⁴² coupling terms with other oscillator (g_{ij}) and a self coupling term (g_{ii}):

$$G_i(X(t)) = \sum_{j=1}^n g_{ij}(X_i(t), X_j(t)) \quad (4)$$

43 then

$$\dot{\varphi}_i = \omega_i + \epsilon \sum_{\substack{j=1 \\ j \neq i}}^n H_{ij}(\varphi_j - \varphi_i, 0) \quad (5)$$

44 with

$$H_{ij}(\varphi_j - \varphi_i, 0) = \frac{1}{T} \int_0^T Q_i(\theta)^T g_{ij}(\gamma_i(\theta), \gamma_j(\theta + \varphi_j - \varphi_i)) d\theta \quad (6)$$

45 and

$$\omega_i = H_{ii}(0, 0) \quad (7)$$

46 *Proof.* Using Eq. 4 in Eq. 3 we have

$$\begin{aligned} H_i(\varphi - \varphi_i, 0) &= \sum_{j=1}^n \frac{1}{T} \int_0^T Q_i(\theta)^T g_{ij}(\gamma_i(\theta), \gamma_j(\theta + \varphi_j - \varphi_i)) d\theta \\ &= \sum_{j=1}^n H_{ij}(\varphi_j - \varphi_i, 0) \end{aligned} \quad (8)$$

47 Then

$$\begin{aligned} \dot{\varphi}_i &= H_i(\varphi - \varphi_i, \epsilon) = \epsilon H_i(\varphi - \varphi_i, 0) = \epsilon \sum_{j=1}^n H_{ij}(\varphi_j - \varphi_i, 0) \\ &= \epsilon H_{ii}(0, 0) + \epsilon \sum_{\substack{j=1 \\ j \neq i}}^n H_{ij}(\varphi_j - \varphi_i, 0) \\ &= \omega_i + \epsilon \sum_{\substack{j=1 \\ j \neq i}}^n H_{ij}(\varphi_j - \varphi_i, 0) \end{aligned} \quad (9)$$

48 The first equality in Eq. 9 follows from Malkin's theorem (Eq. 2), I cannot
 49 understand why the second equality holds, the third equality follows from Eq. 8,
 50 the right-hand side of fourth inequality separates the constant and non-constant
 51 terms in the left-hand side, and the last equality uses Eq. 7.

52

□

53 **Simplification 1.1**

54 **Lemma 1.** *If we take $n = 2$ in Eq. 5 we obtain*

$$\dot{\chi} = \epsilon\omega + \epsilon G(\chi) \quad (10)$$

55 *where*

$$\chi = \varphi_2 - \varphi_1 \quad (11)$$

$$\omega = \omega_2 - \omega_1 \quad (12)$$

$$G(\chi) = H_{21}(-\chi) - H_{12}(\chi) \quad (13)$$

56 *Proof.* Taking $i = 1$ and $i = 2$ in Eq. 5 we obtain

$$\dot{\varphi}_1(t) = \epsilon\omega_1 + \epsilon H_{12}(\varphi_2(t) - \varphi_1(t), 0) \quad (14)$$

$$\dot{\varphi}_2(t) = \epsilon\omega_2 + \epsilon H_{21}(\varphi_1(t) - \varphi_2(t), 0) \quad (15)$$

57 Subtracting Eq. 14 from Eq. 15 and using Eqs. 11-13 we obtain Eq. 10.

58 \square

59 **Note 1** χ is a fixed point of Eq. 10 if and only if $G(\chi) = -\omega$ (Figure 4).

60 **Note 2** If oscillators are not self coupled (i.e., $g_{ii}(\gamma_i(\theta), \gamma_i(\theta)) = 0 \forall i$), then
61 (from Eq. 6) $H_{ii} = 0 \forall i$, then (from Eq. 7) $\omega_i = 0 \forall i$, and then the fixed points
62 of Eq 10 are the zero crossings of $G(\chi)$.

63 **Example**

64 This example attempts to replicate that in Figure 10.26 of Izhikevich (2007). I
65 simulated two two-dimensional low-threshold INap+IK models of neurons (Izhikevich,
66 2007) (Figure 1) with the same parameters used in Figure 10.26 of Izhikevich
67 (2007). The two models shared the same parameters (as given in Figure 4.1b of
68 Izhikevich (2007) and repeated for reproducibility in Table 1), but had differ-
69 ent initial conditions (Tables 2 and 3). The input current to both models was
70 such that when uncoupled these models were on a stable limit cycle ($I_0 = 35$,
71 INap+IK (Class 2) model on Figure 10.3 of Izhikevich (2007) and red traces
72 in Figure 2). These models were weakly coupled with gap junctions (Eq. 16),
73 and the coupling strength was weak enough ($\epsilon = 0.003$ in Eq. 1) so that the
74 coupled models remained close to the uncoupled stable limit cycle (blue traces
75 in Figure 2). The model of neuron 1 (Eq. 17), but not that of neuron 2 (Eq. 18),
76 was self coupled, and below we vary the self-coupling strength of neuron 1 (s in
77 Eq. 17) to obtain different synchronized phase differences between the models
78 of neurons 1 and 2.

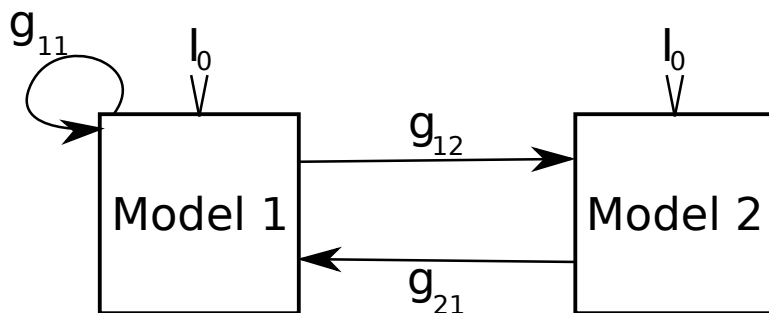


Figure 1: Schema of simulated weakly coupled oscillators. Models 1 and 2 are two-dimensional low-threshold INap+IK models of neurons (Izhikevich, 2007) simulated with the same parameters used in Figure 10.26 of Izhikevich (2007). The two models shared the same parameters (as given in Figure 4.1b of Izhikevich (2007) and repeated for reproducibility in Table 1), but had different initial conditions (Tables 2 and 3). The input current to both models was such that when uncoupled these models were on a stable limit cycle ($I_0 = 35$, INap+IK (Class 2) model on Figure 10.3 of Izhikevich (2007) and red traces in Figure 2). These models were weakly coupled with gap junctions (Eq. 16), and the coupling strength was weak enough ($\epsilon = 0.003$ in Eq. 1) so that the coupled models remained close to the uncoupled stable limit cycle (blue traces in Figure 2). The model of neuron 1 (Eq. 17), but not that of neuron 2 (Eq. 18), was self coupled. Below we vary the self-coupling strength of neuron 1 (s in Eq. 17) to obtain different synchronized phase differences between the models of neurons 1 and 2.

$$g_{ij}(\gamma_i(\theta), \gamma_j(\theta)) = \begin{bmatrix} \gamma_j(\theta)[0] - \gamma_i(\theta)[0] \\ 0 \end{bmatrix}, i \neq j \quad (16)$$

$$g_{11}(\gamma_1(\theta), \gamma_1(\theta)) = \begin{bmatrix} s \times \gamma_1(\theta)[0] \\ 0 \end{bmatrix} \quad (17)$$

$$g_{11}(\gamma_2(\theta), \gamma_2(\theta)) = 0 \quad (18)$$

| Name | Value |
|------------|-------|
| C | 1.0 |
| g_L | 8.0 |
| e_L | -78.0 |
| g_{Na} | 20.0 |
| e_{Na} | 60.0 |
| g_K | 10.0 |
| e_K | -90.0 |
| $mV_{1/2}$ | -90.0 |
| mk | 15.0 |
| $nV_{1/2}$ | -45.0 |
| nk | 5.0 |
| τ | 1.0 |

Table 1: Parameters for the the two INap+IK models of neurons, repeated from Figure 4.1b in Izhikevich (2007).

| Neuron | Name | Value |
|--------|-------|--------|
| 1 | V_0 | -67.42 |
| 1 | n_0 | 0.20 |
| 2 | V_0 | -65.01 |
| 2 | n_0 | 0.16 |

Table 2: Similar set of initial conditions for the two simulated INap+IK models of neurons for voltages, V , and activation gates, n .

| Neuron | Name | Value |
|--------|-------|--------|
| 1 | V_0 | -26.30 |
| 1 | n_0 | 0.50 |
| 2 | V_0 | -65.01 |
| 2 | n_0 | 0.16 |

Table 3: Disimilar set of initial conditions for the two simulated INap+IK models of neurons for voltages, V , and activation gates, n .

79 **4 Problem in Figure 10-26, Panel $I_{Nap}+I_K$ -model**
80 **(Class 2), and in Figure 10-30a, of Izhikevich**
81 **(2007), and Verification of Malkin’s Theorem**

82 I argue that the plots in Figure 10-26, Panel $I_{Nap} + I_K$ -model (Class 2), and
83 in Figure 10-30a, of Izhikevich (2007) are inverted and that the correct figures
84 should be Fig. 3 and Fig. 4.

85 To support this argument I simulated the two weakly-coupled oscillators
86 described in the example of Section 3 with different values of the self-coupling
87 strength of neuron 1, s in Equation 17.

88 A change in s in Equation 17 changes g_{11} in the same equation, which in
89 turn changes H_{11} in Equation 6, which changes ω_1 in Equation 7 and w in
90 Equation 12, which, by Note 1 in Section 3, changes the synchronized phase dif-
91 ference, χ in Equation 11. Thus, according to Malkin’s theorem, simulating the
92 two weakly-coupled oscillators with different values of the self-coupling strength
93 of neuron 1, s in Equation 17, should synchronize these oscillators with different
94 phase differences, χ .

95 The phase difference at which the simulated oscillators synchronize should
96 be at the intercept between $G(\chi)$ and the $-w$ horizontal line (which, as noted
97 above, is a function of the self-coupling strength of neuron 1, s in Equation 17),
98 with $G'(\chi) < 0$ to ensure stability, as shown in Figure 4. Thus, to check if
99 Figures 3 and 4 are correct, I simulated the weakly-coupled oscillators in the
100 Example of Section 3 with different values of self coupling, s in Equation 17,
101 and compared the phase difference at which these simulators synchronized with
102 the intercept of $G(\chi)$ and the $-\omega$ horizontal line in Figure 4.

103 Figure 5 shows results of the simulation of the coupled oscillators in the
104 Example of Section 3 with a self-coupling strenght for oscillator 1 of $s = -3.0$
105 (Equation 17). Initial conditions for both oscillators are shown in Table 2 and
106 were set in such a way that before coupling the phase difference of the oscillators
107 was small ($\chi = 0.3$) and fell in the basin of attraction of the leftmost fixed point
108 in Figure 4. The phase difference of the simulated oscillators in Figure 5 (bottom
109 panel) converged to the leftmost fixed point in Figure 4, suggesting that this
110 figure is correct and that Figure 10.30a of Izhikevich (2007) is not.

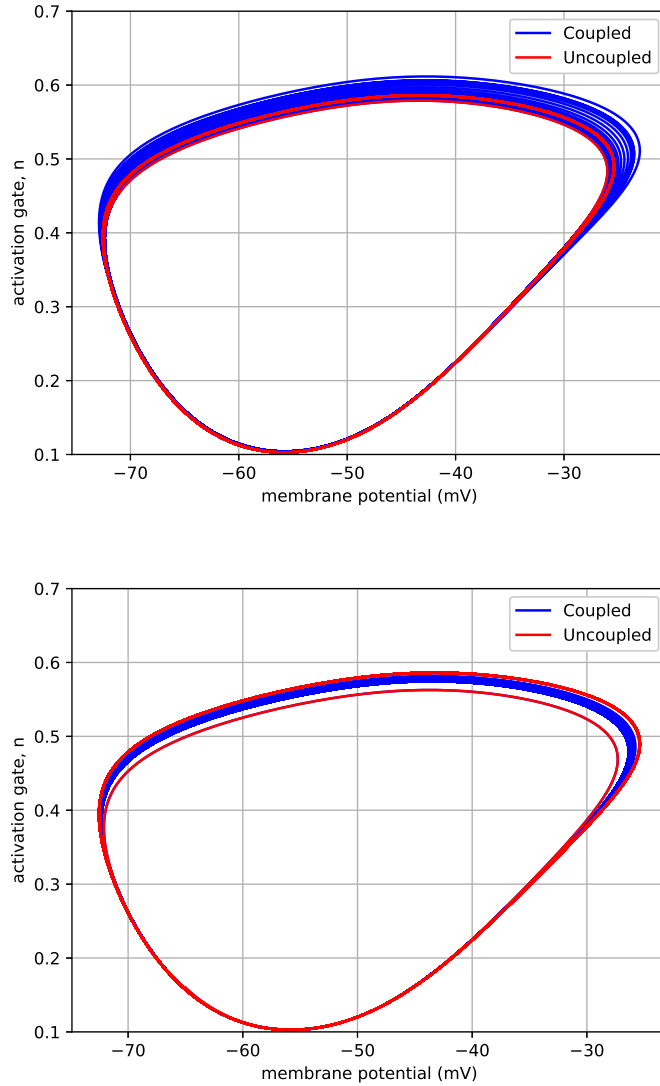


Figure 2: Phase space of the two simulated $I_{Nap} + I_K$ neurons with parameters in Table 1 and the similar initial conditions in Table 2. Top: phase space for neuron 1. Bottom: phase space for neuron 2. Red traces: phase space for uncoupled neuron. Blue traces: phase space for coupled neurons.

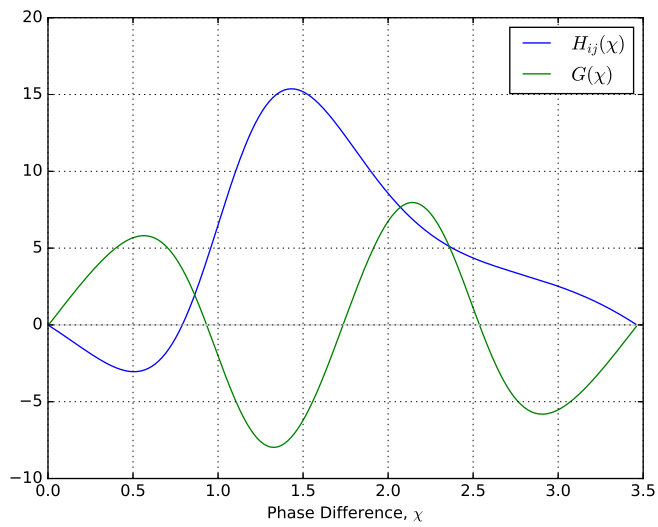


Figure 3: Correct values for the function $G(\chi)$ (Equation 13) and $H_{ij}(\chi)$ (Equation 6) in Figure 10-26 of Izhikevich (2007). Note the change in sign between this figure and Figure 10-26 of Izhikevich (2007). Below we provide evidence suggesting that this figure is correct and Figure 10.26 in Izhikevich (2007) is not.

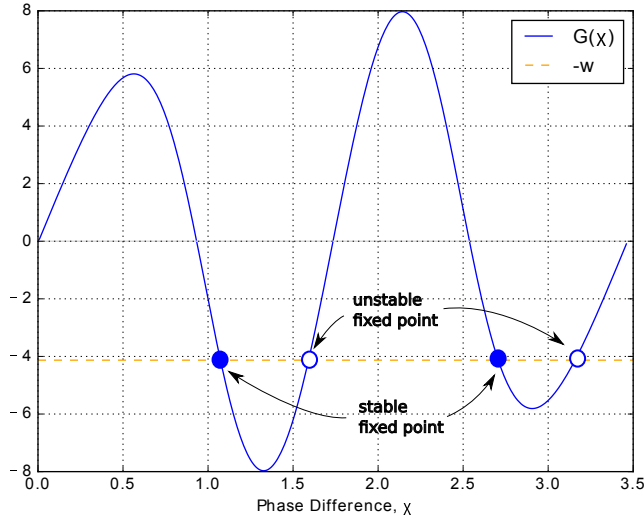


Figure 4: Function $G(\chi)$ (Equation 13), constant $-\omega$ (Equation 12) and fixed points of the phase model in Equation 10 for the coupled oscillators in the Example of Section 3. The self coupling strength for oscillator 1 is $s = -3.0$ (Equation 17). If this figure is correct (and Figure 10.30a of (Izhikevich, 2007) is not) the phase difference of simulated oscillators should converge to the first stable fix point $\chi_{\text{STABLE } 1} = 1.1$ for initial phase differences larger than the second unstable fix point $\chi_{\text{UNSTABLE } 2} = 3.2$ and smaller than the first unstable fix point $\chi_{\text{UNSTABLE } 1} = 1.6$ (see Figure 5). Also, if this figure is correct the phase difference of the oscillators should converge to the second stable fix point $\chi_{\text{STABLE } 2} = 2.7$ for initial phase differences larger than the first unstable fix point $\chi_{\text{UNSTABLE } 1} = 1.6$ and smaller than the second second fix point $\chi_{\text{UNSTABLE } 2} = 3.2$ (see Figure 6).

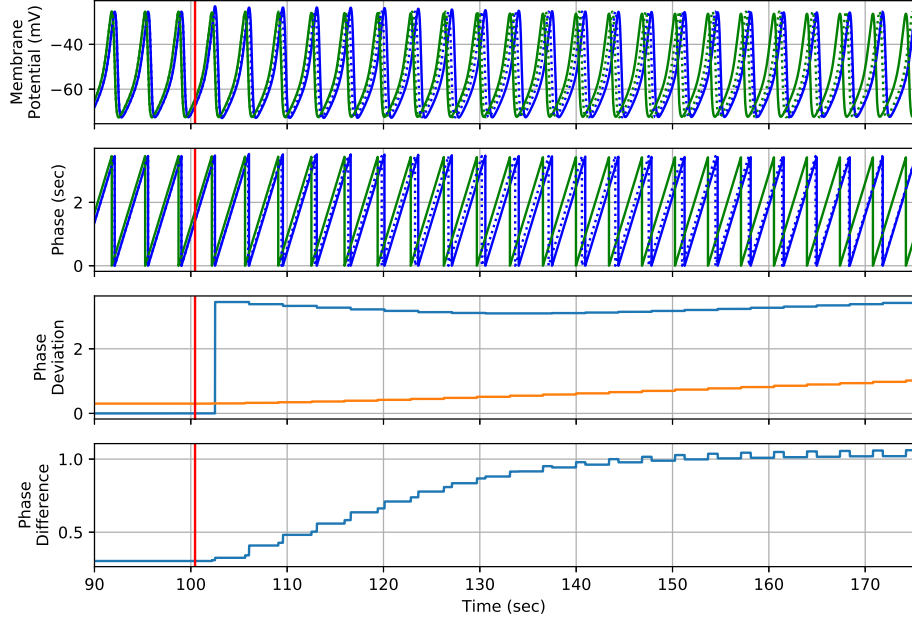


Figure 5: Simulation of the coupled oscillators in the Example of Section 3 with a self-coupling strength for oscillator 1 of $s = -3.0$ (Equation 17) and with a small initial phase difference (similar initial conditions, Table 2). The oscillators become coupled at time 100.44 sec (red vertical line). The top panel plots the simulated membrane potential of oscillators zero (blue lines) and one (green lines). Solid and dashed lines plot membrane potentials of coupled and uncoupled oscillators, respectively. The second panel from the top plots the phase of the coupled oscillators and that of uncoupled oscillator zero. The third panel plots the deviation of the phase of a coupled oscillator with respect to the phase of the same oscillator when uncoupled. The bottom panel shows the difference of the phase deviation of oscillator one minus that of oscillator zero. This simulation corresponds to the phase model depicted in Figure 4. Initial conditions for both oscillators were set in such a way that before the coupling the phase of the oscillators were similar ($\chi = 0.3$). After coupling the phase of the oscillators start to diverge and the oscillators become synchronized at a phase difference $\chi = 1.1$ around 150 sec. This simulation supports the correctness of Figure 4 (and suggest an error in Figure 10.30a of Izhikevich (2007)). The initial phase difference of the oscillators $\chi = 0.3$ was on the basin of attraction of the stable fixed point at phase difference $\chi = 1.1$ in Figure 4, and the phase difference of the simulated oscillators converged to this value.

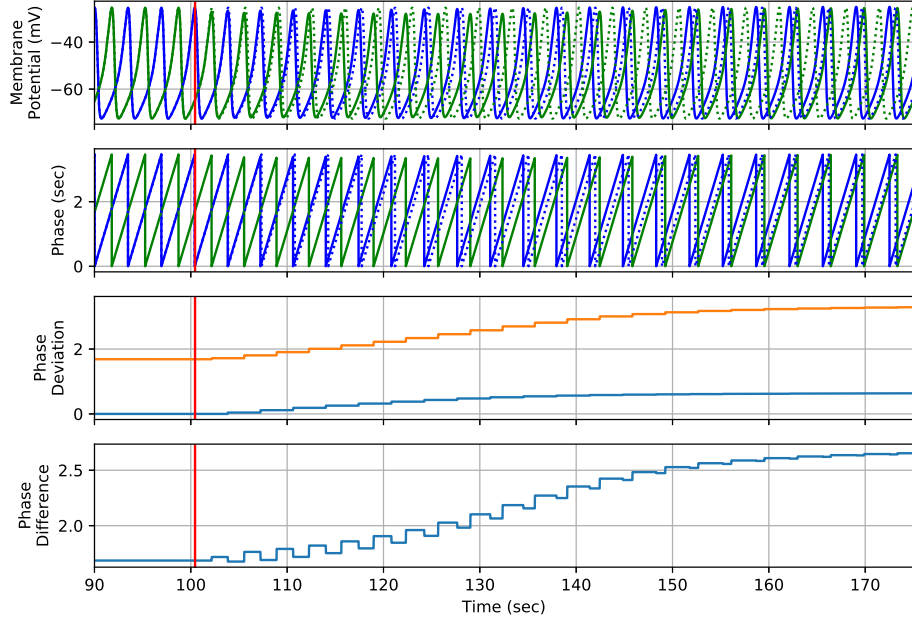


Figure 6: Simulation of the coupled oscillators in the Example of Section 3 with a self-coupling strength for oscillator 1 of $s = -3.0$ (Equation 17) and with a large initial phase difference (disimilar initial conditions, Table 3). This simulation corresponds to the phase model depicted in Figure 4. Same format as in Figure 5. Initial conditions for both oscillators were set in such a way that before the coupling the phase of the oscillators were different ($\chi = 1.7$). After coupling the phase of the oscillators start to diverge more and the oscillators become synchronized at a phase difference $\chi = 2.7$ around 180 sec. This simulation supports the correctness of Figure 4. The initial phase difference of the oscillators $\chi = 1.7$ was on the basin of attraction of the stable fixed point at phase difference $\chi = 2.7$ in Figure 4, and the phase difference of the simulated oscillators converged to this value.

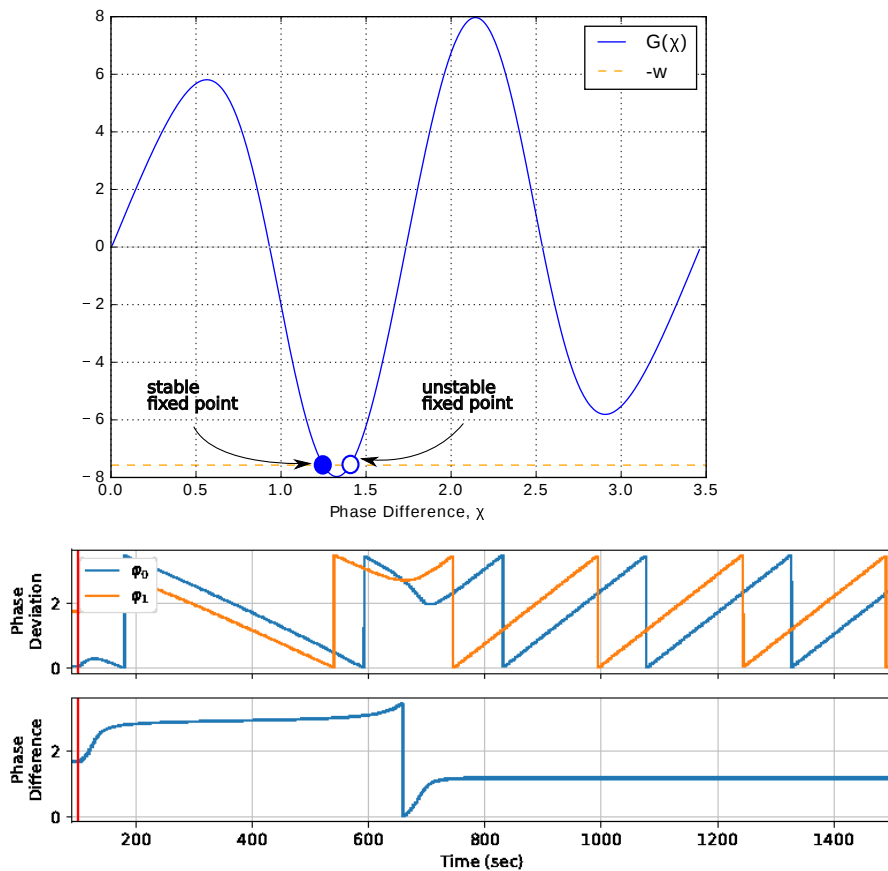


Figure 7: Phase model (top panel) and simulation (bottom panel) of the coupled oscillators in the Example of Section 3 with a self-coupling strength for oscillator 1 of $s = -5.5$ (Equation 17). Same format as in Figure 5. Top panel: the self-coupling strength of oscillator 1 yields a small value of $-w$ and the horizontal line at $-w$ intercepts the $G(\chi)$ curve at only one pair of points corresponding to stable and an unstable fixed points. Bottom panel: after coupling the oscillators their phase difference almost gets trapped by the ghost of the saddle noise bifurcation at $\chi = 2.9$ and later converge to the stable fixed point at $\chi = 1.2$. Table 3 gives the initial conditions used for this simulation. This simulation supports the correctness of Figure 4.

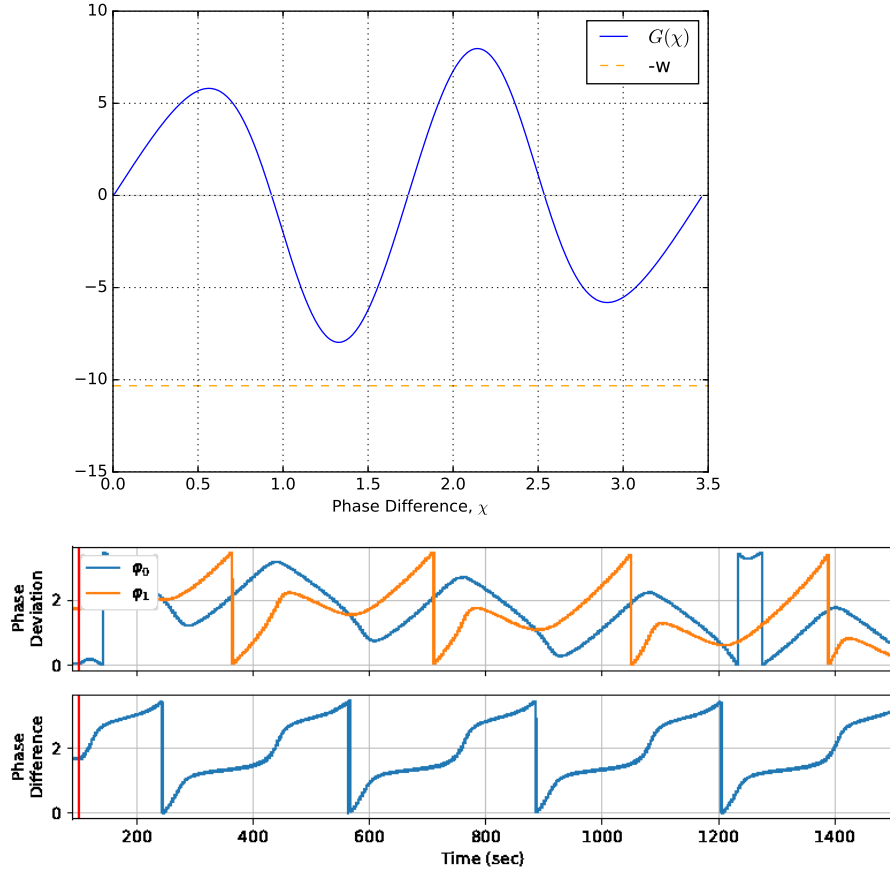


Figure 8: Phase model (top panel) and simulation (bottom panel) of the coupled oscillators in the Example of Section 3 with a self-coupling strength for oscillator 1 of $s = -7.5$ (Equation 17). Same format as in Figure 5. Top panel: the self-coupling strength of oscillator 1 yields a very small value of $-w$, the horizontal line at $-w$ does not intercept the $G(\chi)$ curve, and there are not stable fixe points. Bottom panel: after coupling the phase difference of the simulated oscillators keeps fluctuating and does reach a stable value. Table 3 gives the initial conditions used for this simulation. This simulation supports the correctness of Figure 4 and the incorrectness of Figure 10-26, panel $I_{Nap} + I_K$ -model (Class 2) and of Figure 10-30a, of Izhikevich (2007).

111 **References**

- 112 Hoppensteadt, F. C., & Izhikevich, E. M. (1997). *Weakly connected neural*
113 *networks* (Vol. 126). Springer Science & Business Media.
- 114 Izhikevich, E. M. (2007). *Dynamical systems in neuroscience*. MIT press.